ORIGINAL RESEARCH PAPER

Preparation and application of collagen scaffold-encapsulated silver nanoparticles and bone morphogenetic protein 2 for enhancing the repair of infected bone

Chang-ying Sun · Yan-jun Che · Shi-jin Lu

Abstract The healing of contaminated/infected bone defects is a significant clinical challenge. Here, a novel collagen scaffold composite encapsulating silver nanoparticles (AgNP) and bone morphogenetic protein 2 (BMP-2) was prepared to enhance the healing of infected bone defects. Collagen scaffolds conjugated with AgNP possessed strong antibacterial properties that were dependent on the release rate of Ag^+. After introducing BMP-2, the BMP-2/AgNP/collagen scaffold composites did not adversely affect the adherence or proliferation of bone marrow-derived mesenchymal stromal cells (BMSCs). Differentiation of BMSCs toward osteoblasts was induced by the upregulation of RUNX2, osteopontin and osteonectin expression. BMP-2/AgNP/collagen scaffold composites, therefore, possess the antibacterial activity of AgNP and the osteoinductivity of BMP-2, making these composites an ideal pharmaceutical for the regeneration of bone in infected wounds.

Introduction

Bone tissue engineering is a promising approach for treating bone loss resulting from trauma or bone diseases (Burg et al. 2000; Bos et al. 2012). Despite the rapid development of bone tissue engineering, the prevention of significant bone loss in a non-sterile wound still poses a challenge due to the extremely long and complicated healing process of contaminated and infected bone defects (Guelcher et al. 2011; Nguyen et al. 2013). In fact, 2–10 % of implanted bone grafts used in large-area bone loss surgeries, such as open fractures, combat-related injuries and revision joint replacements, can increase the incidence of host infection (Belt et al. 2001). Therefore, the development of novel bone grafts that are capable of simultaneously controlling infections and promoting bone regeneration would be advantageous.

Compared to current antibiotics, silver (Ag) is resistant to a wider range of bacteria because it binds to and disrupts multiple components related to bacterial structure and metabolism (Lansdown 2002). With the rapid development of nanotechnology, Ag nanoparticles (AgNP) are attracting increasing attention because of their larger surface-to-mass ratio, greater

Chang-ying Sun and Yan-jun Che have contributed equally to this work.

C. Sun · Y. Che (✉)
Department of Orthopedics, Peace Hospital Affiliated to Changzhi Medical College, Changzhi 046000, Shanxi, China
e-mail: cyj789@163.com

S. Lu
Department of Spine Surgery, Xiangya Hospital of Central South University, Changsha 10008, Hunan, China

solubility and chemical reactivity and higher antibacterial activity compared to traditional silver agents (Alt et al. 2004). Thus, AgNP appear to be promising for use in healing bone graft infections. Furthermore, bone morphogenetic protein 2 (BMP-2) has been demonstrated to be a strong osteoinductive factor, and it has previously been used for the treatment of many bone fractures and bone defects (Li et al. 2006; Bessa et al. 2008). Therefore, bone grafts incorporating both AgNP and BMP-2 have the potential to be an ideal scaffold for use in treating bone infections. The purpose of this study was to create a novel multifunctional nanosystem that includes BMP-2 and AgNP as an adjunctive therapy for infected segmental bone defects. This novel multifunctional bone graft, which combines the advantages of BMP-2, AgNP and collagen, will be a better treatment option for bone tissue engineering, particularly for the repair of large-area bone loss.

Materials and methods

Preparation and characterization of bone morphogenic protein 2 (BMP-2)/silver nanoparticles (AgNP)/collagen scaffolds

Collagen scaffold-encapsulated AgNP were synthesized using a modification of the method of Xie et al. (2009). Briefly, 5 ml 10 mM $AgNO_3$ was added to 250 mg collagen powder in 5 ml distilled water with vigorous stirring at room temperature. Approximately. 0.3 ml 1 M NaOH was added, followed by the addition of 10 mM $NaBH_4$ to form the AgNP/collagen solution. Encapsulation of AgNP and BMP-2 by the collagen solution was achieved via the addition of 100 μl 10 μg ml^{-1} BMP-2 solution. Finally, collagen scaffold-encapsulated AgNP and BMP-2 were obtained through lyophilization via freeze-drying. The freshly prepared products were characterized using scanning electron microscopy (SEM), transmission electron microscopy (TEM) and X-ray diffraction (XRD).

In vitro antimicrobial activity

Vancomycin-resistant *Staphylococcus aureus* Mu50 (ATCC 700699) was used in a bacterial infection model. In vitro testing of the antimicrobial activity was performed using a broth microdilution method (Espinel-Ingroff et al. 2011). *S. aureus* was dispersed in ultrapure water to give 10^5 c.f.u. ml^{-1}. Then, 50 μl of the dispersion was seeded in a 96-well microplate that contained 100 μl of double-concentration nutrient broth in each well. To the wells, 50 ml aliquots of diluted suspensions of collagen, AgNP/collagen and BMP-2/AgNP/collagen scaffolds were added. The final concentrations of collagen, AgNP/collagen and BMP-2/AgNP/collagen scaffolds were 0.1, 0.2, 0.5, 1.5, 2.5, 5 and 10 μg ml^{-1}. Pure broth without nanoparticle treatment (200 ml) served as the negative control. After incubating aerobically at 37 °C for 24 h, the OD_{595} values of the seeded cells were measured using a microplate reader. The minimum inhibitory concentration (MIC) is defined as the minimum concentration of the compound required to completely inhibit bacterial growth after incubation at 35 °C for 24 h.

Ion release from AgNP

Approximately the same equivalents of AgNP/collagen solution, BMP-2/AgNP/collagen solution and $AgNO_3$ solution were added to 10 ml ultrapure water and mixed to form homogeneous solutions. The solutions were transferred to dialysis tubes and immersed in 100 ml ultrapure water. The dialysis was conducted with slow stirring at 35 °C. At intervals, the concentration of Ag^+ was analyzed by dialysis and inductively coupled plasma (ICP) atomic emission spectrometry.

Cell isolation, seeding and culturing on scaffolds

Bone marrow-derived mesenchymal stromal cells (BMSCs) were isolated from bone marrow aspirates according to Sun et al. (2010). Bone marrow aspirates were mixed with complete culture medium that contained low-glucose Dulbecco's Modified Eagle's Medium, 15 % (v/v) fetal bovine serum and 1 % antibiotics (200 units penicillin G ml^{-1} and 200 units streptomycin sulfate ml^{-1}) and then cultured at 37 °C under a humidified 5 % CO_2 atmosphere. The cultures were replenished with fresh medium every 3–4 days. BMSCs were isolated by selective adherence to the polystyrene tissue culture dish, and non-adherent cells were removed by changing the medium and subculturing. Semi-confluent cells of the second passage (P2)

were used for seeding the scaffolds. A BMSC cell suspension was dispensed drop-wise onto the surface of each scaffold at 2.5×10^5 cells. The cell-seeded scaffolds were incubated for 2 h at 37 °C with 5 % (v/v) CO_2 to allow the cells to adhere to the scaffolds. Following incubation, 2 ml fresh medium was added to each well to cover both the cell-seeded and negative control scaffolds. The culture plates were then incubated at 37 °C with 5 % (v/v) CO_2. The osteoinductivity and osteoconductivity of the BMP-2/AgNP/collagen scaffold were evaluated by seeding with the BMSCs and compared to the osteoinductivity and osteoconductivity of the collagen and AgNP/collagen scaffolds. The scaffolds were sterilized by autoclaving and were seeded with BMSCs at 1.5×10^5 cells per scaffold. The cell-seeded scaffolds were cultured in a 5 % (v/v) CO_2 incubator at 37 °C, and the medium was replaced every 3 days.

MTT assay

A modified MTT test, in which yellow MTT is reduced to purple formazan crystals by dehydrogenases in cells, was used to assess cell viability. After 1, 3 or 7 days of incubation in different media, the viability of the BMSCs was assessed. Briefly, the BMSCs were washed three times with culture medium. 100 μl 5 mg MTT ml^{-1} was added to the culture medium in each well of the plate. After incubation for 4 h at 37 °C, the reaction solution was carefully removed from each well, and then 200 μl dimethyl sulfoxide was added. The plates were gently agitated until the formazan precipitate dissolved, and then the A_{490} values were measured with a microplate reader.

DNA content analysis

At various times, collagen, AgNP/collagen and BMP-2/AgNP/collagen scaffolds were washed in phosphate buffered saline (PBS) and then lysed in 0.2 % (w/v) Triton X-100 and 5 mM $MgCl_2$. The Pico Green assay was used to measure the total amount of DNA fluorometrically with excitation at 480 nm and emission at 528 nm.

Gene expression analysis by quantitative RT-PCR

The expression levels of the genes encoding various proteins involved in osteogenesis, such as runt-related transcription factor 2 (RUNX2), alkaline phosphatase (ALP), osteopontin and osteonectin, were analyzed in the BMSC-seeded scaffolds. During the culture period, total RNA was extracted from the scaffolds of each group (n = 3) at several time intervals using an RNeasy Kit. Quantitative reverse transcription PCR (qRT-PCR) was performed with β-actin as the reference gene. The primer sequences of the genes were obtained from the literature. ALP activity was determined by using an ALP assay kit.

Statistical analysis

The results are graphically depicted as the mean and the standard deviation (SD). A two-tailed t test and one-way ANOVA were performed (SPSS 13.0 for Windows, SPSS, Chicago, IL) to detect statistically significant differences. $p < 0.05$ was considered to be statistically significant.

Results and discussion

The preparation and characterization of bone morphogenic protein 2 (BMP-2)/silver nanoparticles (AgNP)/collagen scaffolds

Proteins are a good template for preparing nanoparticles in an aqueous phase because it is easy to conjugate metal ions with the amino acid residues of proteins via affinity interactions (Kong et al. 2010, 2013; Chen et al. 2012, 2013). Collagen, which has the natural biological composition of bone, is also a suitable template for synthesizing AgNP. The TEM image (Fig. 1a) indicated that the AgNP in the collagen solution were spherical with sizes ranging from 10 to 50 nm. A single AgNP with clear lattice fringes was observed in the HR-TEM image (Fig. 1b), and its size was approximately. 20 nm. As shown in Fig. 1c, the SEM image revealed that the collagen scaffold contained a porous network. Notably, after surface modification with an AgNP coating, the surface of the collagen scaffolds was very coarse. Furthermore, the XRD pattern of as-prepared product (Fig. 1d) showed that all of the AgNP peaks matched well with the standard XRD pattern of silver powder (JCPDS 04-0783), indicating that our product was composed of crystalline Ag. Moreover, these as-prepared collagen scaffolds that encapsulated both
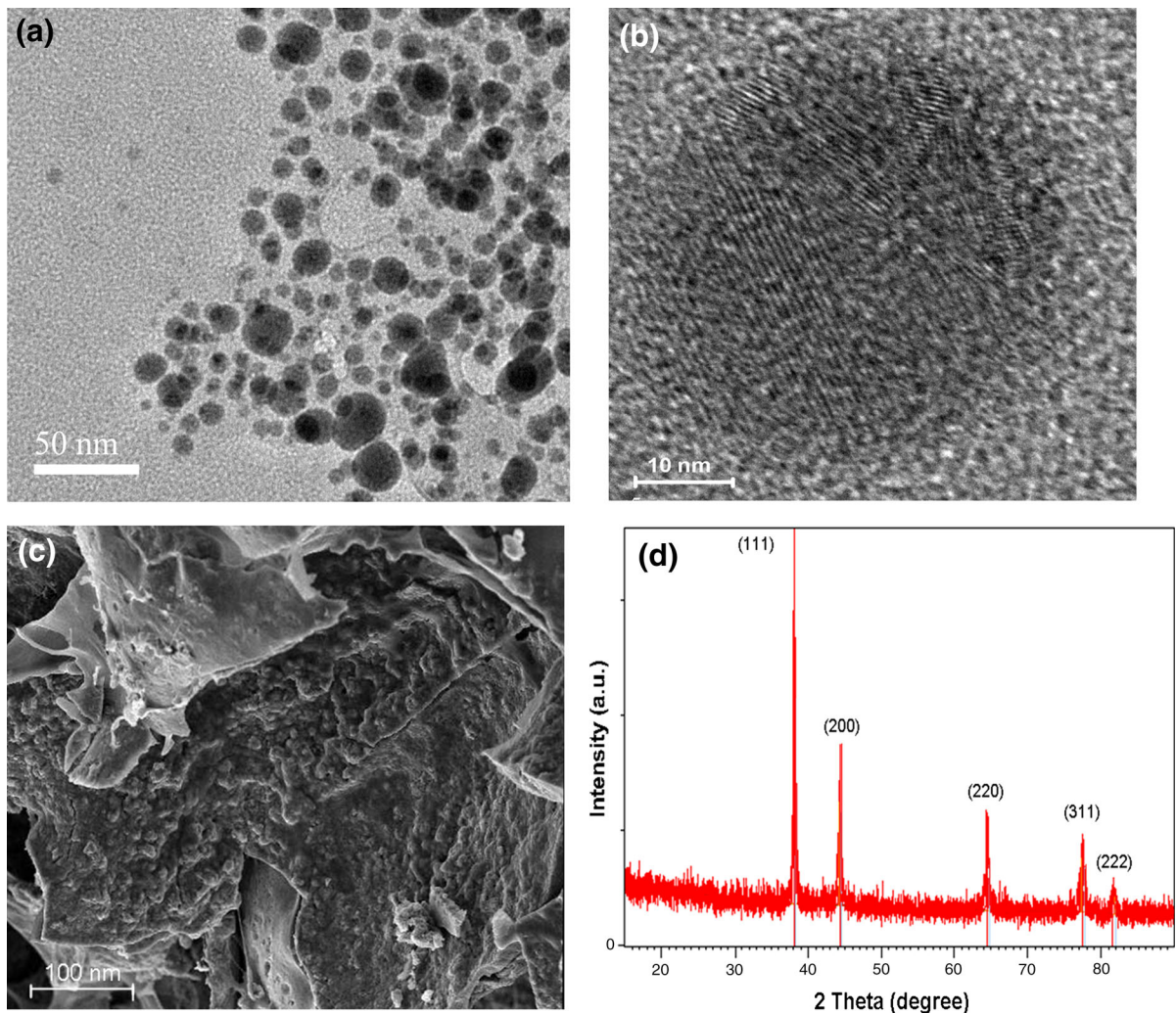
Fig. 1 **a** Typical TEM image of as-prepared collagen solution containing AgNP. **b** HR-TEM image of a single Ag nanoparticle in the collagen solution. **c** SEM image of the surface of BMP-2/AgNP/collagen scaffolds. **d** XRD pattern of freshly prepared BMP-2/AgNP/collagen scaffolds

AgNP and BMP-2 were stable for three months, and no aggregation was observed. This stability may result from the cross-linking between collagen, AgNP and BMP-2, which provides a protein layer to resist the degradation of BMP-2 and oxidation of Ag NPs.

Antibacterial activity of AgNP

As shown in Fig. 2a, the absorbance of *S. aureus* Mu50 remained relatively high in the presence of different concentrations of collagen scaffolds, even when the concentration of the collagen scaffold reached 10 µg ml^{-1}. Thus, collagen scaffolds did not inhibit the growth of *S. aureus*. Because collagen itself is not osteogenic or antibacterial, it is not an ideal candidate for repairing infected bone. However, the MIC of both the AgNP/collagen samples and the BMP-2/AgNP/collagen samples against *S. aureus* Mu50 was approx. 0.1 µg ml^{-1}. Furthermore, as the concentration increased to 10 µg ml^{-1}, the proliferation of *S. aureus* Mu50 in both the AgNP/collagen samples and the BMP-2/AgNP/collagen samples was completely inhibited in vitro, indicating that the AgNP retained their original antibacterial activity against *S. aureus* Mu50 after being encapsulated in the collagen scaffolds.
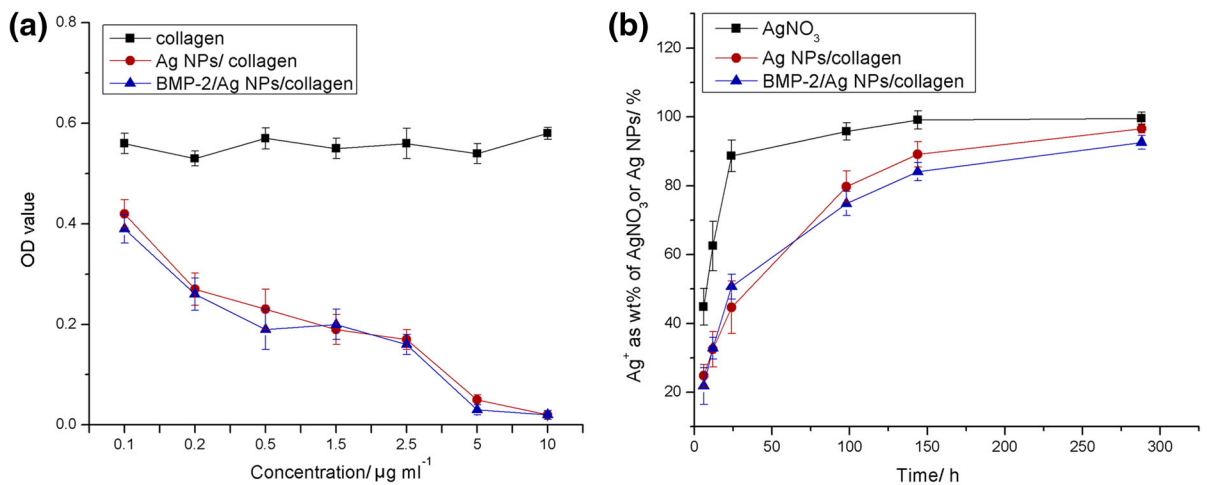
Fig. 2 **a** Tests of the antibacterial activities of collagen, AgNP/collagen and BMP-2/Ag NP/collagen against *Staphylococcus aureus* Mu50 at different concentrations using the broth microdilution method. **b** Ag$^+$ release curves of AgNO$_3$, AgNP/collagen and BMP-2/AgNP/collagen at 35 °C

Ag$^+$ release

The duration of antibacterial activity of AgNP complexes generally depends on the duration of Ag$^+$ release. Thus, the antibacterial properties of AgNP complexes are enhanced with longer periods of Ag$^+$ release. As shown in Fig. 2b, our prepared BMP-2/AgNP hybrid collagen scaffolds had a longer Ag$^+$ release period than other Ag composite nanosystems described in previous studies, such as Ag–carbene complexes (Hindi et al. 2009), SiO$_2$/polydopamine/Ag nanocomposites (Dong et al. 2014), chitosan/AgNP/polyvinyl alcohol complexes (Abdelgawad et al. 2012) and chitosan-Ag/polyvinylpyrrolidone nanocomposites (Wang et al. 2012). Specifically, in our study, most of the Ag$^+$ was released in a "burst" in the first 24 h, with approx. 45 and 50.5 % of the Ag$^+$ being released from the AgNP/collagen and BMP-2/AgNP/collagen groups, respectively. At the same time, approx. 89 % of the Ag$^+$ was rapidly released from the AgNO$_3$ sample into the aqueous phase. After the burst release phase, a slow release was sustained for the Ag$^+$ complex groups. One potential reason for this behavior is that the collagens present on the surface of the AgNP may serve as a steric barrier that retards the diffusion of AgNP from the scaffolds. Alternatively, the sustained release of AgNP may result from the slow degradation of the collagen scaffolds.

Cell viability and proliferation

An evaluation of the viability of the BMSCs using MTT assays and DNA content analyses also indicated that the seeded BMSCs proliferated and remained viable for 7 days of culturing on the scaffolds (Figs. 3a, b). As shown in Fig. 3a, only a slight difference was observed in the proliferation rate of BMSCs on the scaffolds during the 7 day culture period, which indicated that either AgNP or BMP-2 could affect the proliferation of BMSCs seeded on the scaffolds. Similarly, there was no significant difference with respect to the DNA content in those scaffolds (Fig. 3b), as the average DNA concentrations were 15.21 ± 1.35, 22.31 ± 1.51 and 30.25 ± 2.21 ng scaffold^{-1} on day 1, 3 and 7, respectively. Accordingly, the average DNA concentrations for the AgNP/collagen scaffold were 17.05 ± 2.58, 22.75 ± 1.37, and 31.21 ± 3.18 ng scaffold^{-1} on day 1, 3 and 7, and the values for the BMP-2/AgNP/collagen scaffold were 16.54 ± 2.58, 24.31 ± 1.61, and 33.25 ± 2.18 ng scaffold^{-1} on day 1, 3 and 7, respectively.

Gene expression analysis by quantitative RT-PCR

Bone-related genes, such as osteopontin and osteonectin, have been implicated as markers of osteogenic differentiation. These genes are expressed early in the differentiation process, and their expression persists
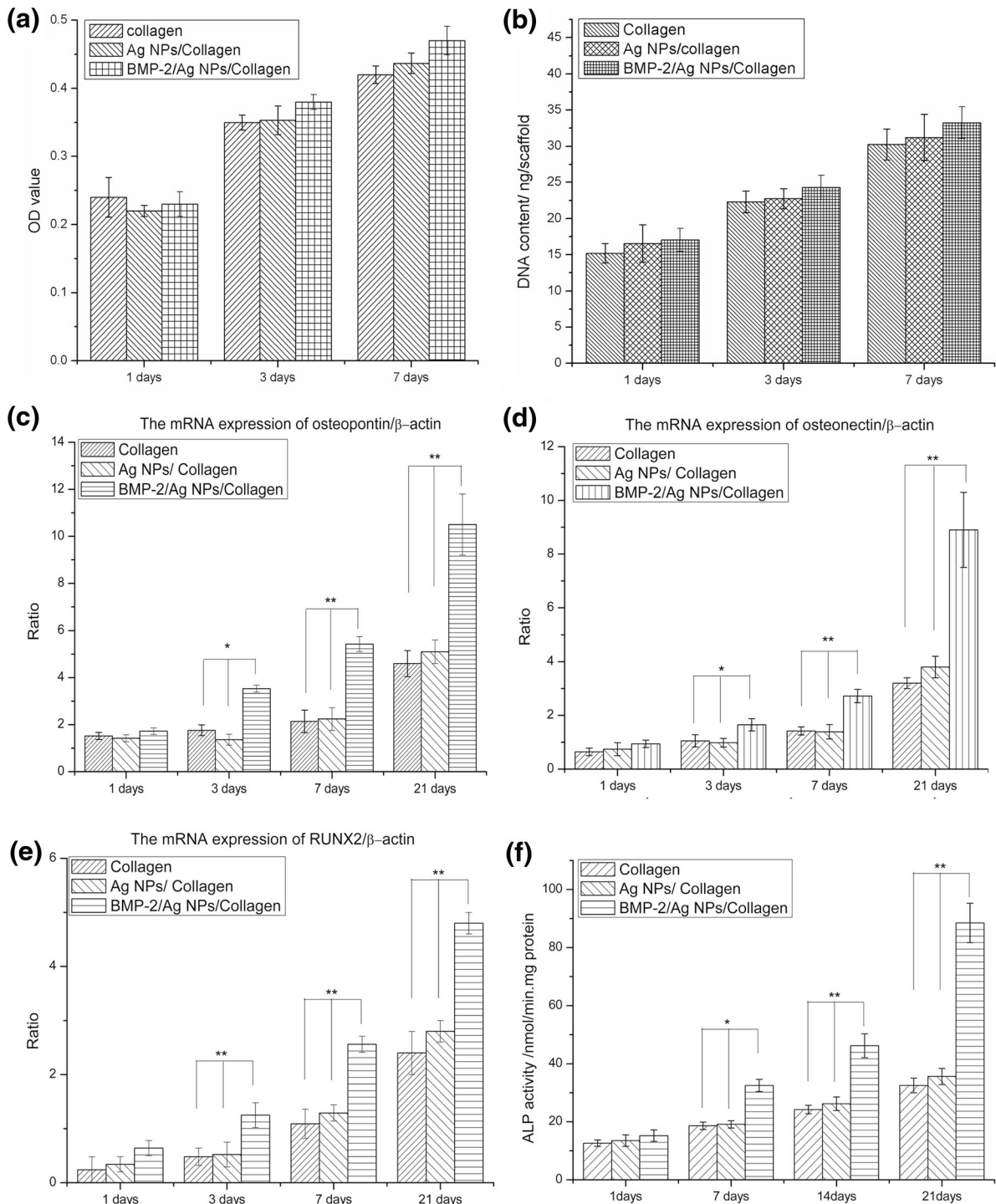
Fig. 3 **a** MTT and **b** DNA content analyses to determine the viability of BMSCs co-cultured with collagen, AgNP/collagen and BMP-2/AgNP/collagen for 1, 3 and 7 days. mRNA expression analyses of **c** osteopontin, **d** osteonectin and **e** RUNX2 as well as analysis of **f** ALP activity in collagen, AgNP/collagen and BMP-2/AgNP/collagen scaffolds for 1, 3, 7 and 21 days. The data represent the mean ± SD; *$p < 0.05$; **$p < 0.01$; n = 6 for each sample

throughout the maturation of osteoblasts. As shown in Fig. 3c–f, the mRNA expression analyses of BMSC-seeded BMP-2/AgNP/collagen scaffolds after 7 days of culture showed significant upregulation of RUNX2, osteopontin and osteonectin as well as increased ALP activity compared with the BMSC-seeded collagen scaffolds and AgNP/collagen scaffolds. These observations implied that BMP-2 encapsulated in AgNP/collagen scaffolds could retain the ability to induce the differentiation of BMSCs toward osteoblasts.

Conclusion

Multifunctional BMP-2/AgNP hybrid collagen scaffolds were prepared that simultaneously combined the porous structure of collagen scaffolds, the antibacterial activity of AgNP and the osteoinductivity of the BMP-2 protein. The hybrid structure of AgNP and collagen increased the surface roughness of the scaffold and provided a 3D matrix for the adhesion and proliferation of BMSCs. Compared with collagen scaffolds, the as-prepared BMP-2/AgNP/collagen scaffolds enhanced the differentiation of BMSCs toward osteoblasts. The prepared scaffolds, however, still lack sufficient mechanical strength for bone repair (data not shown) and this will be addressed in our future studies. However, our study clearly demonstrates the potential of multifunctional BMP-2/AgNP/collagen hybrid scaffolds for repairing infected bone.

References

Abdelgawad AM, Hudson SM, Rojas OJ (2012) Antimicrobial wound dressing nanofiber mats from multicomponent (chitosan/silver-NPs/polyvinyl alcohol) systems. Carbohyd Polym 100:166–178

Alt V, Bechert T, Steinrücke P, Wagener M, Seidel P, Dingeldein E, Domann E, Schnettler R (2004) An in vitro assessment of the antibacterial properties and cytotoxicity of nanoparticulate silver bone cement. Biomaterials 25:4383–4391

Belt H, Neut D, Schenk W, Horn JR, Mei HC, Busscher HJ (2001) Infection of orthopedic implants and the use of antibiotic-loaded bone cements: a review. Acta Orthop Scand 72:557–571

Bessa PC, Casal M, Reis RL (2008) Bone morphogenetic proteins in tissue engineering: the road from laboratory to clinic, part II (BMP delivery). J Tissue Eng Regen Med 2:81–96

Bos S, Roy M, Bandyopadhyay A (2012) Recent advances in bone tissue engineering scaffolds. Trends Biotechnol 30:546–554

Burg KJ, Porter S, Kellam JF (2000) Biomaterial developments for bone tissue engineering. Biomaterials 21:2347–2359

Chen J, Zhang T, Feng LL, Zhang X, Zhang MQ, Cui DX (2012) Synthesis of ribonuclease A-conjugated CdS quantum dots and its photocatalytic properties. Micro Nano Lett 7:1023–1025

Chen J, Zhang T, Feng LL, Zhang MQ, Zhang X, Su HC, Cui DX (2013) Synthesis of ribonuclease A-conjugated Ag$_2$S quantum dots clusters via biomimetic route. Mater Lett 96:224–227

Dong Y, Liu T, Sun SB, Chang XT, Guo N (2014) Preparation and characterization of SiO2/polydopamine/Ag nanocomposites with long-term antibacterial activity. Ceram Int 40:5605–5609

Espinel-Ingroff A, Fothergill A, Fuller J, Johnson E, Pelaez T, Turnidge J (2011) Wild-type MIC distributions and epidemiological cutoff values for caspofungin and Aspergillus spp. for the CLSI broth microdilution method (M38-A2 document). Antimicrob Agent Chemother 55:2855–2859

Guelcher SA, Brown KV, Li B, Guda T, Lee BH, Wenke JC (2011) Dual-purpose bone grafts improve healing and reduce infection. J Orthop Trauma 25:477–482

Hindi KM, Ditto AJ, Panzner MJ, Medvetz DA, Han DS, Hovis CE, Hilliard JK, Taylor JB, Yun YH, Cannon CL, Youngs WJ (2009) The antimicrobial efficacy of sustained release silver–carbene complex-loaded L-tyrosine polyphosphate nanoparticles: characterization, in vitro and in vivo studies. Biomaterials 30:3771–3779

Kong YF, Chen J, Gao F, Li WT, Xu X, Pandoli O, Yang H, Ji JJ, Cui DX (2010) A multifunctional ribonuclease-A-conjugated CdTe quantum dot cluster nanosystem for synchronous cancer imaging and therapy. Small 6:2367–2373

Kong YF, Chen J, Gao F, Brydson R, Johnson B, Heath G, Zhang Y, Wu L, Zhou DJ (2013) Near-infrared fluorescent ribonuclease-A-encapsulated gold nanoclusters: preparation, characterization, cancer targeting and imaging. Nanoscale 5:1009–1017

Lansdown A (2002) Silver I: its antibacterial properties and mechanism of action. J Wound Care 11:125–131

Li C, Vepari C, Jin HJ, Kim HJ, Kaplan DL (2006) Electrospun silk-BMP-2 scaffolds for bone tissue engineering. Biomaterials 27:3115–3124

Nguyen H, Cassady AI, Bennett MB, Gineyts E, Wu A, Morgan DAF, Forwood MR (2013) Reducing the radiation sterilization dose improves mechanical and biological quality while retaining sterility assurance levels of bone allografts. Bone 57:194–200

Sun X, Xia L, Chou LL, Zhong W, Zhang X, Wang S, Zhao J, Jiang X, Zhang Z (2010) Maxillary sinus floor elevation using a tissue engineered bone complex with BMP-2 gene modified bMSCs and a novel porous ceramic scaffold in rabbits. Arch Oral Biol 55:195–202

Wang BL, Liu XS, Ji Y, Ren KF, Ji J (2012) Fast and long-acting antibacterial properties of chitosan-Ag/polyvinylpyrrolidone nanocomposite films. Carbohyd Polym 90:8–15

Xie J, Zheng Y, Ying JY (2009) Protein-directed synthesis of highly fluorescent gold nanoclusters. J Am Chem Soc 131:888–889